Second Harmonic Generation Dynamics in Plasmonic Nanoparticles

Gabriel D. Bernasconi*, Jérémy Butet, Olivier J. F. Martin
Nanophotonics and Metrology Laboratory, Swiss Federal Institute of Technology Lausanne (EPFL), 1015 Switzerland

ABSTRACT

Due to its symmetry properties, second-harmonic generation in plasmonic nanostructures enables the observation of even-parity modes that couple weakly to the far field. Consequentially, those modes radiate less and thus have a longer lifetime. Using a full-wave numerical method, we study the linear and second harmonic dynamical responses of a silver nanorod under plane-wave femtosecond pulse illumination. Depending on the spectral position and duration of the pulse, the decaying field of the different modes can be separated, and the free oscillations of each mode are well fitted by a damped harmonic oscillator model, both in the linear and nonlinear regimes. Additionally, interference effects between different modes excited at the second harmonic are observed.

Keywords: SHG, dynamics, eigenmodes, ultrafast

1. INTRODUCTION

The coherent oscillation of free electrons in metals is known to enable a strong localization of the electromagnetic field.[1-3] Those plasmonic resonances can be spectrally tuned by changing the shape and geometry of the nanoparticle(s) and exhibit a strong dependence on the material and surrounding medium properties.[4, 5] The large concentration of surface charges around metallic nanoparticles allows reaching extreme field intensities that can then enhance nonlinear processes. One of the many applications of such a field enhancement is the generation of harmonics. Indeed, nonlinear mechanisms depend on higher power of the intensity and thus benefit from the large intensity found on plasmonic nanoparticles. Among all nonlinear processes, second harmonic (SH) generation (SHG) has received particular attention from the plasmonic community.[6, 7] The importance of the eigenmode structure of nanoparticles for an efficient SHG has been put forward with the design of double resonant nanostructures.[8-12] Additionally, eigenmode-oriented studies of the SHG have also been conducted in order to reveal their influence at both the fundamental and nonlinear stages.[13-15] Nevertheless, the dynamics of the SHG, especially the response of nanostructures to femtosecond pulses has not yet been addressed in detail, even though this is of great importance for the coherent control of SH light and for temporal measurements techniques relying on nonlinear processes.

In this paper we extend the study conducted in ref [16] to a more detailed analysis of the interference between dipole and quadrupole at the second harmonic wavelength for short pulse illumination. We show that the SH field can be observed to behave like a damped harmonic oscillator for specific pulse durations and widths, and reveal the dynamical interference between two, or more, eigenmodes.

2. THEORY

The simulations are made using a full-wave method in the frequency domain, namely the surface integral equation method (SIE).[17, 18] One considers only the surface of the nanoparticle that is discretized into triangular elements and, by enforcing the boundary conditions of the field, one can solve for equivalent currents on the surface. The time harmonic dependence of the field is of the form $e^{-i\omega t}$, with $i = \sqrt{-1}$, ω the angular frequency in rad·s^{-1} and t the time in s. Throughout the manuscript we use electronvolts (eV) units to express ω, i.e. $\omega = h\nu/q_0$ with ν the frequency in Hz, q_0 the elementary charge, and h Planck's constant.

To build a signal with a finite duration, more than one frequency is needed. Thus, the second order nonlinear process will

*gabriel.bernasconi@epfl.ch

Plasmonics: Design, Materials, Fabrication, Characterization, and Applications XVI, edited by Din Ping Tsai, Takuo Tanaka, Proc. of SPIE Vol. 10722, 107221U · © 2018 SPIE
CCC code: 0277-786X/18/$18 · doi: 10.1117/12.2321004

lead to sum-frequency generation (SFG) in addition to second-harmonic generation.[19] We neglect the difference frequency generation and optical rectification processes. For two complex harmonic fields $E_1(t)$ and $E_2(t)$ of the form $E_m(t) = e^{-i\omega_m t}$, the second order nonlinear polarization $P^{(2)}(t)$ is [19]

$$P^{(2)}(t) = P_{2\omega_1} e^{-i\omega_1 t} + P_{2\omega_2} e^{-i\omega_2 t} + P_{\omega_1+\omega_2} e^{-i(\omega_1+\omega_2)t}, \quad (1)$$

with $P_{2\omega_1} = \epsilon_0 \chi^{(2)} E_1^2$, $P_{2\omega_2} = \epsilon_0 \chi^{(2)} E_2^2$ and $P_{\omega_1+\omega_2} = 2\epsilon_0 \chi^{(2)} E_1 E_2$ respectively the SHG (twice) and the SFG. $\chi^{(2)}$ is the nonlinear susceptibility tensor. The second order nonlinearity $\chi^{(2)}$ is considered to exist only on the surface of the nanoparticle where the centrosymmetry is broken. Additionally, the only non-vanishing component of the nonlinear susceptibility tensor is assumed to be $\chi^{(2)}_{\perp\perp\perp}$,[20-22] where the subscript $\perp$ indicates the component perpendicular to the surface. The method used in ref [23] and [24] is modified to include the nonlinear polarization of the SFG. In practice, $\chi^{(2)}_{\perp\perp\perp}$ is small enough so that one can neglect any back transfer of energy from the nonlinear polarization to the linear signal, and we make the undepleted pump approximation. Finally, the relative amplitude of the linear and nonlinear signal is of no importance here, so, without loss of generality, we set $\chi^{(2)}_{\perp\perp\perp} = 1$.

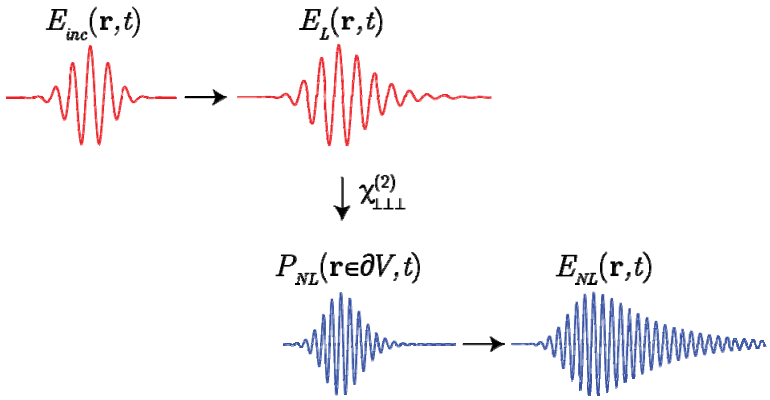

Figure 1. Temporal SFG computation. The incoming excitation E_{inc} is used to compute the linear response E_L that is in turn used to compute the nonlinear surface sources P_{NL}. These sources are then used to obtain the nonlinear response. Each step is computed in the frequency domain and the temporal signals are constructed by inverse Fourier transform.

The femtosecond pulses are defined in the frequency domain by the frequency envelop

$$S(\omega) = e^{-(\omega-\omega_0)^2/2\Delta\omega^2}, \quad (2)$$

with ω_0 the central frequency and $\Delta\omega$ the width. The Fourier transform of $S(\omega)$ gives a temporal signal of the same Gaussian form, with width $\Delta t = 2\pi/\Delta\omega$. The corresponding full width at half maximum is $FWHM = 2\sqrt{2\ln(2)}\Delta t \cong 2.35\Delta t$.

Since computations can be made only for a finite amount of frequencies, the associated temporal signal will have a period $T = 2\pi/\delta\omega$, with $\delta\omega$ the constant frequency step between each frequency. For the results to be meaningful, this period must be larger than the longest observable dynamic of interest. Plasmon's lifetime are known to be of the order of ~10 fs and we choose a frequency step of $\delta\omega$=0.02 eV, leading to a period $T = 207$ fs.

Eigenmodes of the nanorod are obtained by looking at poles of the nanostructure response in the complex frequency plane .[25, 14] The permittivity of the silver is obtained by a Drude model with the following parameters: ω_p=9.3 eV, γ=0.03 eV and ε_∞=4.3, with ω_p the plasma frequency, γ the damping constant and ε_∞ the permittivity for $\omega\to\infty$. The refractive index of the surrounding medium is set to n=1.33. Due to radiative and damping losses, the eigenfrequencies are complex, $\omega_c = \omega_r + i\omega_i$, with the real part being related to the resonant frequency and the imaginary part to the

damping rate. When there is no external excitation of the system, all the quantities $A(t)$ associated with an eigenmode evolve freely according to the harmonic dependence $\mathrm{Re}\{e^{-i\omega_c t}\}$, thus leading to

$$A(t) \propto \cos(\omega_r t) e^{\omega_i t}. \quad (3)$$

This temporal evolution is analogous to that of a damped harmonic oscillator.[26] We can then expect that when the excitation pulse dies out, the free evolution of the eigenmodes can be observed given that their lifetime is longer than the pulse duration and that their resonant frequency is close to the pulse central one.

3. RESULTS

3.1 Second harmonic response and eigenmodes

The eigenmode analysis reveals that the three modes of interest are the longitudinal dipole and quadrupole and the transverse dipole. The longitudinal dipole, which is responsible for most of the linear response, has a real frequency of 1.74 eV and a lifetime of 7.03 fs. Thus, the linear harmonic response shows a single peak at 1.74 eV (data not shown). The longitudinal quadrupole has a central frequency of 2.8 eV and a lifetime of 27 fs, whereas the transverse quadrupole has a central frequency of 3.38 eV and a lifetime of 3.93 fs. The large difference in lifetime between the three modes is explained by their properties: the quadrupole is weakly coupled to the far-field, and thus loses energy at a small rate. Comparatively, the dipolar modes are strongly damped due to their energy leaking efficiently to the far-field. Lastly, the transverse quadrupole is needed as an intermediate step at the fundamental stage to account for the SH dipolar emission, but its dynamics is not observable in the following analysis. The eigenfrequencies and associated quantities of the above-mentioned eigenmodes are summarized in Table 1.

We first present the SHG from the silver nanorod for a harmonic plane wave at normal incidence and polarized along the long axis of the nanorod, Fig. 2. The first small peak at 2.8 eV (notice the scaling by a factor 100) corresponds to the resonance of the longitudinal quadrupolar mode at the SH frequency. The second peak at 3.5 eV is due to the resonance of the longitudinal dipole at the linear stage at 1.74 eV. A multipolar analysis[27] reveals that the first peak is indeed mainly quadrupolar but has a non-negligible dipolar contribution as well. Indeed, the large damping rate associated with the transverse dipolar resonance makes its spectral response relatively large, allowing it to respond to frequency well below 3.38 eV.

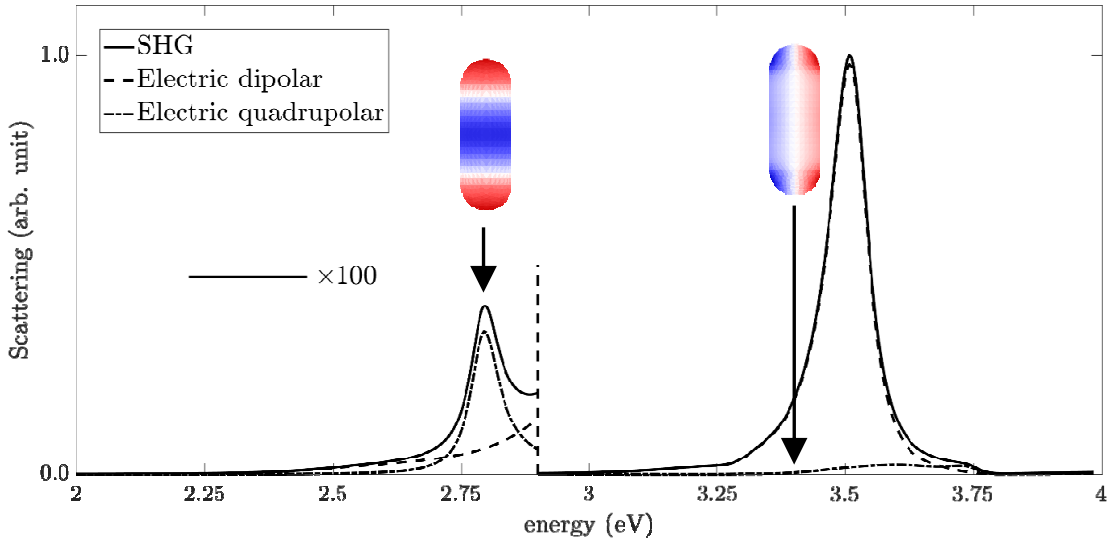

Figure 2. Second harmonic spectrum and eigenmodes. The spectrum is decomposed into dipolar and quadrupolar radiative components. The eigenfrequencies of the longitudinal quadrupole and transverse dipole are indicated with black arrows.

Table 1. Eigenfrequencies, lifetimes and quality factors $Q = \omega_r/|\omega_i|$

	ω_r (eV)	ω_i (eV)	τ (fs)	Q
Long. dipole	1.74	-0.0936	7.03	18.5
Long. quadrupole	2.80	-0.0244	27.0	115
Trans. quadrupole	3.27	-0.0418	15.7	78.3
Trans. dipole	3.38	-0.168	3.93	20.1

3.2 Pulse excitation, nonlinear response

We now consider the second harmonic response of the nanorod to a short pulse centered at half the resonance of the longitudinal quadrupole, i.e. 1.4 eV. The E_y field is probed at three points in the far-field at a distance of 10μm, namely at ±45° and at 0° (y=0, see Fig. 3(a)). Two different pulse widths are considered: 0.14 and 0.21 eV, respectively corresponding to FWHM of 11 and 7 fs. We first study the longer pulse, i.e. the spectrally narrower one. The field in the ±45° directions shows two distinct regimes, Fig. 3(b). In the first part t < 55fs, interferences are observed. As already reported in the literature,[28, 29] this effect is due to the interference between the longitudinal quadrupole and the transverse dipolar modes. Here the interference is constructive in the -45° direction (green curve) and destructive in the +45° direction (red curve). Let us remark however that this will depend on the relative spectral position of both modes as well as the pulse central frequency. To prove that the above-mentioned mechanism is at play here, we compute the sum of the fields at the ±45° points. Since they should be out of phase without any interference, this sum reveals the disturbance and is plotted with black markers on the bottom part. We now plot the field in the 0° direction (blue curve) as it should only be linked to the dipolar resonance since the quadrupole does not radiate in that direction. It is observed that the dipolar trace indeed matches the sum of the field in the ±45° direction, confirming the interference effect between the two modes. Let us note that the almost perfect match between the blue curve and black symbol is fortuitous and is the result of the relative amplitude of the dipolar and quadrupolar radiation patterns in the ±45° directions as well as the intrinsic amplitude of each mode. We also note that the field at +45° presents a beating-like pattern during the interference.

For times larger than ~55 fs, the interference vanishes, Fig. 3(b). This is because the transverse dipolar mode is no longer oscillating. Indeed, its lifetime, 3.93 fs, is shorter than the pulse width, 11 fs, so that it dies out with the driving pulse. On the other hand, the lifetime of the longitudinal quadrupole is comparatively longer, 27 fs, and one can indeed observe a free oscillation of the fields in the ±45° directions. Furthermore, with the parameters of the longitudinal quadrupole given in Table 1, we fit Eq. (3) to the green curve, see black curve in inset in Fig. 3(b). It is apparent that the match between the damped harmonic oscillator model and the free oscillation and the field obtained with full wave computation is very good.

If we now look at the case of a shorter pulse excitation, Fig. 3(c), we observe a more complex interference pattern. This is because the pulse is spectrally broad enough to excite higher order modes that have dipolar-like radiation pattern and symmetry. We thus observe a beating in the dipolar response due to the interference between (at least two) dipolar modes. However, the sum of the fields in the +45° directions still matches the dipolar trace, showing that the interference effect observed in the previous case also occurs when more than two modes are excited at the second harmonic wavelength. We can also note that the higher order dipolar-like mode has a lifetime large enough to create interferences well after the excitation pulse has vanished.

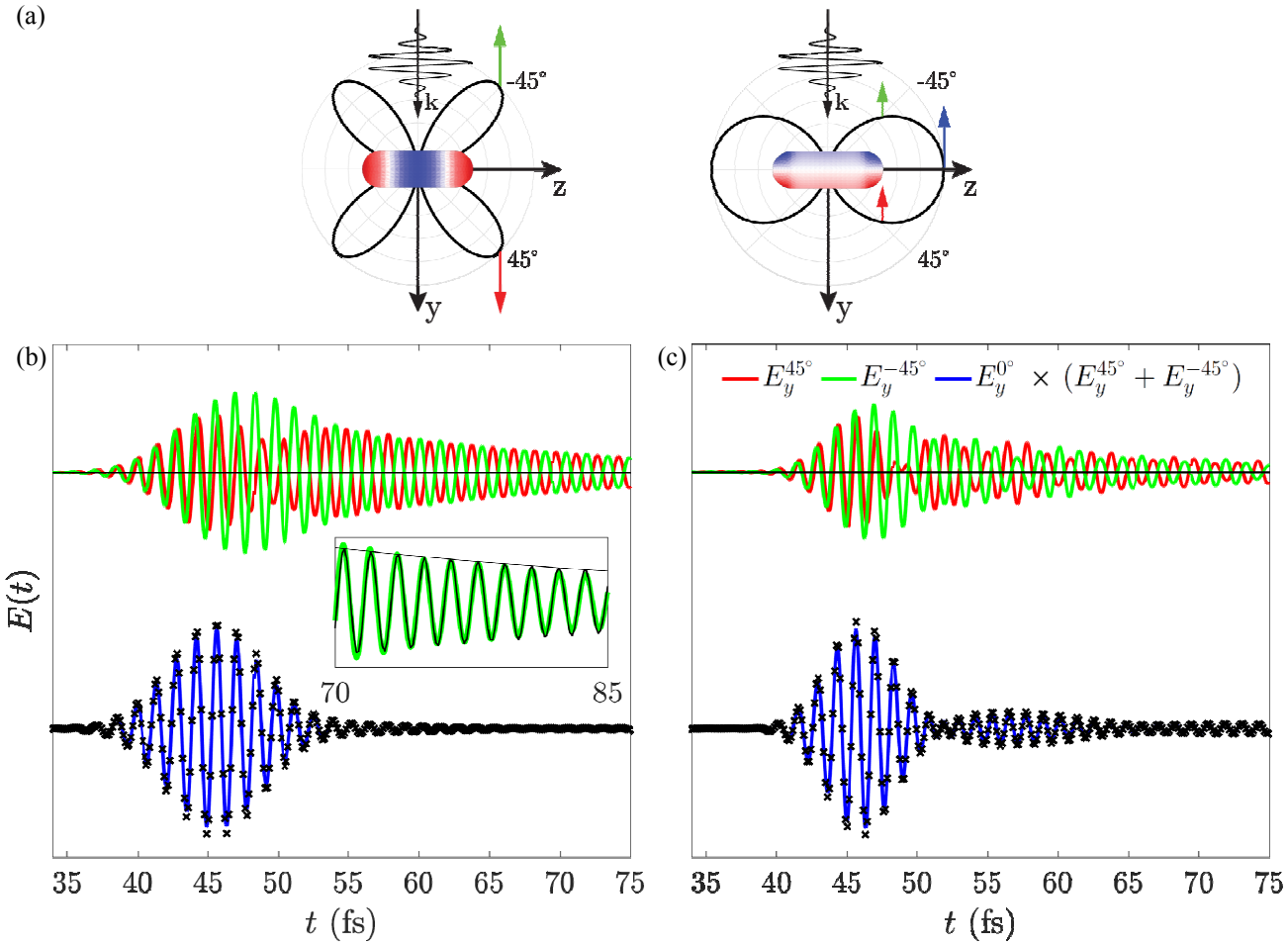

Figure 3. Farfield (10 μm) second harmonic response of the nanorod. (a) Radiation pattern of the longitudinal quadrupole and transverse dipole excited at the SH and indication of the field orientation at the points of interest. (b) Pulse of width 0.14 eV. Electric field in +45°, -45° and 0° respectively in red, green and blue. The black markers are the sum of the red and green curves. The inset shows the field at -45° fitted with Eq. (3). (c) Same as in (b) for a pulse of width 0.21 eV.

4. CONCLUSION

The dynamics of the second harmonic generation in a plasmonic silver nanorod has been studied for short pulse excitation. For the longest pulse, it has been shown that the interference between the longitudinal and quadrupolar modes occurs only during the time where the excitation is driving the structure, due to the very short lifetime of the transverse dipolar mode. In subsequent times, the longitudinal quadrupole resonance evolves freely, with a dynamic matching the one of a damped harmonic oscillator. For a shorter pulse, the corresponding spectral broadening allows the excitation of higher order modes of dipolar character. We thus observe a beating like interference between such high order modes and the transverse dipolar one. This dipolar component again interferes with the quadrupolar radiation and creates a more complicated interference between both types of modes. Those results reveal that the modal structure of the system studied is of importance when considering the nonlinear dynamics of the response at the femtosecond scale and that, accordingly, the response may strongly vary with the pulse central frequency and width.

ACKNOWLEDGEMENTS

Funding from the Swiss National Science Foundation (project 200020_153662) and from the European Research Council (ERC-2015-AdG-695206 Nanofactory) is gratefully acknowledged.

REFERENCES

[1] Barnes, W. L., Dereux, A., Ebbesen, T. W. "Surface plasmon subwavelength optics," Nature 2003, 424, 824.
[2] Schuller, J. A., Barnard, E. S., Cai, W., Jun, Y. C., White, J. S., Brongersma, M. L. "Plasmonics for extreme light concentration and manipulation," Nat. Mater. 9, 193 (2010)
[3] Kottmann, J. P., Martin, O. J., Smith, D. R., Schultz, S. "Dramatic localized electromagnetic enhancement in plasmon resonant nanowires," Chem. Phys. Lett, 341, 1−6 (2001).
[4] Liz-Marzán, L. M., "Tailoring Surface Plasmons through the Morphology and Assembly of Metal Nanoparticles," Langmuir 22, 32−41 (2006).
[5] Halas, N. J., Lal, S., Chang, W.-S., Link, S., Nordlander, P., "Plasmons in Strongly Coupled Metallic Nanostructures," Chem. Rev. 111, 3913−3961 (2011).
[6] Kauranen, M., Zayats, A. V., "Nonlinear plasmonics," Nat. Photonics 6, 737 (2012).
[7] Butet, J., Brevet, P.-F., Martin, O. J. F., "Optical Second Harmonic Generation in Plasmonic Nanostructures: From Fundamental Principles to Advanced Applications," ACS Nano 9, 10545−10562 (2015).
[8] Thyagarajan, K.; Rivier, S.; Lovera, A.; Martin, O. J. F., "Enhanced second-harmonic generation from double resonant plasmonic antennae," Opt. Express 20, 12860−12865 (2012).
[9] Aouani, H., Navarro-Cia, M., Rahmani, M., Sidiropoulos, T. P. H., Hong, M., Oulton, R. F., Maier, S. A., "Multiresonant Broadband Optical Antennas As Efficient Tunable Nanosources of Second Harmonic Light," Nano Lett. 12, 4997−5002 (2012).
[10] Celebrano, M., Wu, X., Baselli, M., Großmann, S., Biagioni, P., Locatelli, A., De Angelis, C., Cerullo, G., Osellame, R., Hecht, B., Duò, L., Ciccacci, F., Finazzi, M., "Mode matching in multiresonant plasmonic nanoantennas for enhanced second harmonic generation," Nat. Nanotechnol. 10, 412 (2015).
[11] Ethis de Corny, M., Chauvet, N., Laurent, G., Jeannin, M., Olgeirsson, L., Drezet, A., Huant, S., Dantelle, G., Nogues, G., Bachelier, G., "Wave-Mixing Origin and Optimization in Single and Compact Aluminum Nanoantennas," ACS Photonics 3, 1840−1846 (2016).
[12] Yang, K.-Y., Butet, J., Yan, C., Bernasconi, G. D., Martin, O. J. F., "Enhancement Mechanisms of the Second Harmonic Generation from Double Resonant Aluminum Nanostructures," ACS Photonics 4, 1522−1530 (2017).
[13] Butet, J., Dutta-Gupta, S., Martin, O. J. F., "Surface second-harmonic generation from coupled spherical plasmonic nanoparticles: Eigenmode analysis and symmetry properties," Phys. Rev. B: Condens. Matter Mater. Phys. 89, 245449 (2014).
[14] Bernasconi, G. D., Butet, J., Martin, O. J. F., "Mode analysis of second-harmonic generation in plasmonic nanostructures," J. Opt. Soc. Am. B 33, 768 (2016).
[15] Smirnova, D., Smirnov, A. I., Kivshar, Y. S., "Multipolar Second-Harmonic Generation by Mie-Resonant Dielectric Nanoparticles," Phys. Rev. A: At., Mol., Opt. Phys. 97, 013807 (2018).
[16] Bernasconi, G.D., Butet J., and Martin O. J. F., "Dynamics of Second-Harmonic Generation in a Plasmonic Silver Nanorod," ACS Photonics, article ASAP (2018)
[17] Kern, A. M., Martin, O. J. F., "Surface integral formulation for 3D simulations of plasmonic and high permittivity nanostructures," J. Opt. Soc. Am. A 26, 732−740 (2009).
[18] Raziman T. V., Somerville W. R., Martin O. J. F., Le Ru E. C., "Accuracy of surface integral equation matrix elements in plasmonic calculation," J. Opt. Soc. Am. B 32, 485-492 (2015)
[19] Boyd, R. W. Nonlinear Optics, Academic Press, (2003).
[20] Krause, D., Teplin, C. W., Rogers, C. T., "Optical Surface Second Harmonic Measurements of Isotropic Thin-Film Metals: Gold, Silver, Copper, Aluminum, and Tantalum," J. Appl. Phys. 96, 3626−3634 (2004).
[21] Wang, F. X., Rodríguez, F. J., Albers, W. M., Ahorinta, R., Sipe, J. E., Kauranen, M., "Surface and bulk contributions to the second-order nonlinear optical response of a gold film," Phys. Rev. B: Condens. Matter Mater. Phys. 80, 233402 (2009).

[22] Bachelier, G., Butet, J., Russier-Antoine, I., Jonin, C., Benichou, E., Brevet, P.-F., "Origin of optical second-harmonic generation in spherical gold nanoparticles: Local surface and nonlocal bulk contributions," Phys. Rev. B: Condens. Matter Mater. Phys. 82, 235403 (2010).
[23] Mäkitalo, J., Suuriniemi, S., Kauranen, M., "Boundary element method for surface nonlinear optics of nanoparticles," Opt. Express 19, 23386−23399 (2011).
[24] Butet, J., Gallinet, B., Thyagarajan, K., Martin, O. J. F., "Second-harmonic generation from periodic arrays of arbitrary shape plasmonic nanostructures: a surface integral approach," J. Opt. Soc. Am. B 30, 2970−2979 (2013).
[25] Bai, Q., Perrin, M., Sauvan, C., Hugonin, J.-P., Lalanne, P., "Efficient and intuitive method for the analysis of light scattering by a resonant nanostructure," Opt. Express 21, 27371 (2013).
[26] Faggiani, R., Losquin, A., Yang, J., Mårsell, E., Mikkelsen, A., Lalanne, P., "Modal Analysis of the Ultrafast Dynamics of Optical Nanoresonators," ACS Photonics 4, 897−904 (2017).
[27] Mühlig, S., Menzel, C., Rockstuhl, C., Lederer, F., "Multipole analysis of meta-atoms," Metamaterials 5, 64−73 (2011).
[28] Butet, J., Raziman, T., Yang, K.-Y., Bernasconi, G. D., Martin, O. J., "Controlling the nonlinear optical properties of plasmonic nanoparticles with the phase of their linear response," Opt. Express 24, 17138 (2016).
[29] Butet, J., Bernasconi, G. D., Petit, M., Bouhelier, A., Yan, C., Martin, O. J. F., Cluzel, B., Demichel, O., "Revealing a Mode Interplay That Controls Second-Harmonic Radiation in Gold Nanoantennas," ACS Photonics 4, 2923−2929 (2017).